
baller2vec++: A Look-Ahead Multi-Entity Transformer For Modeling Coordinated Agents

Michael A. Alcorn

Department of Computer Science and Software Engineering
Auburn University
Auburn, AL 36849
alcorma@auburn.edu

Anh Nguyen

Department of Computer Science and Software Engineering
Auburn University
Auburn, AL 36849
anh.ng8@gmail.com

Abstract

In many multi-agent spatiotemporal systems, the agents are under the influence of shared, *unobserved* variables (e.g., the play a team is executing in a game of basketball). As a result, the trajectories of the agents are often statistically *dependent* at any given time step; however, almost universally, multi-agent models implicitly assume the agents’ trajectories are statistically *independent* at each time step. In this paper, we introduce `baller2vec++`, a multi-entity Transformer that can effectively model coordinated agents. Specifically, `baller2vec++` applies a specially designed self-attention mask to a *mixture* of location and “look-ahead” trajectory sequences to learn the distributions of statistically dependent agent trajectories. We show that, unlike `baller2vec` (`baller2vec++`’s predecessor), `baller2vec++` can learn to emulate the behavior of perfectly coordinated agents in a simulated toy dataset. Additionally, when modeling the trajectories of professional basketball players, `baller2vec++` outperforms `baller2vec` by a wide margin.

1 Introduction and Related Work

Whether it is a team executing a play in a game of basketball, a family navigating to an attraction in a theme park, or friends posting about a birthday party on a social media platform, humans frequently coordinate their behavior in response to shared information. When this coordinating information is unobserved (which is often the case in many machine learning datasets), the individuals’ observed behaviors become correlated, i.e., the behavior of one individual at a specific time contains information about the behavior of another individual *at the same time*. In the context of forecasting agent trajectories in multi-agent spatiotemporal systems, this property translates to the trajectories being statistically dependent at each time step. However, nearly all multi-agent spatiotemporal models (e.g., [1–6]) implicitly (through their loss functions) assume the trajectories of the agents at each time step are statistically *independent* given the agents’ previous locations (Figure 1).

¹All data and code for the paper are available at: <https://github.com/airalcorn2/baller2vecplusplus>.

Zhan et al. [7] explicitly focused on modeling coordinated multi-agent trajectories, using “macro-intents” [8] that are shared across agents to do so.

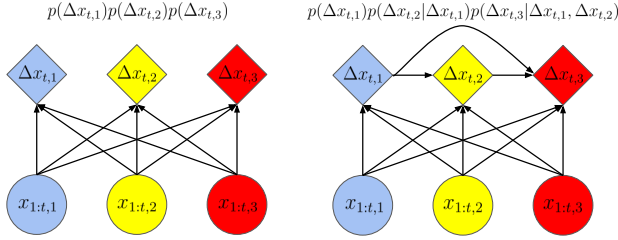


Figure 1: **Left:** most multi-agent systems implicitly assume the trajectories of the agents at each time step ($\Delta x_{t,k}$) are conditionally independent given the agents’ previous positions ($x_{1:t,k}$). **Right:** however, the various decompositions of the joint probability of the trajectories, e.g., $p(\Delta x_{t,1})p(\Delta x_{t,2}|\Delta x_{t,1})p(\Delta x_{t,3}|\Delta x_{t,1}, \Delta x_{t,2})$ (note, we omit the conditional $x_{1:t,k}$ terms for brevity), suggest more complex statistical dependencies between the agents’ trajectories can exist (i.e., the independence assumption is an extremely strong one). Indeed, there are often shared unobserved variables influencing the spatiotemporal behaviors of agents—such as the play that the players on a basketball team are executing, or events occurring in a pedestrian environment—which suggests statistical dependencies between the agents’ trajectories are likely.

The macro-intents are generated from a separately trained recurrent neural network (RNN) that learns to predict a future, coarse, “stationary” location for each agent at each time step. The macro-intents for all of the agents at a specific time step are concatenated together to form a single, shared, macro-intent variable, which is then provided as input to the trajectories-generating model at that time step. However, similar to the previously mentioned multi-agent trajectory models, the macro-intents model implicitly assumes the macro-intents for the agents at each time step are statistically independent, i.e., the generated macro-intent for one agent does not depend on the generated macro-intents of the other agents.² Further, the trajectories-generating model still implicitly assumes the trajectories of the agents at each time step are independent, which is only true if the shared macro-intent variable perfectly captures all of the unobserved information that could cause the agents’

trajectories to be correlated.

Notably, Social-BiGAT [9] *does* partially account for trajectory correlations through a global adversarial loss. Specifically, the trajectories for each agent are separately passed through an encoder RNN, and the final hidden states for each agent are then processed with a graph attention network (GAT) [10]. The output of the GAT is then used as an input to a discriminator that classifies whether or not the input trajectories are real or generated. This global adversarial loss, however, is only a single component of the full Social-BiGAT loss function, and other components of the loss function *do* implicitly make the independence assumption. Further, interestingly, adding the global discriminator to a baseline model only improved the model’s performance for one out of six pedestrian datasets.

In this paper, we describe a novel multi-agent spatiotemporal model that integrates information about *concurrent* actions of agents to predict statistically dependent distributions of trajectories. Specifically, we extend the recently introduced multi-entity Transformer `baller2vec` [6] by: (1) augmenting its input with a parallel sequence of “look-ahead” agent trajectories and (2) using a specially designed self-attention mask, which allows our model to exploit the chain rule of probability (Section 3). We find that:

1. `baller2vec++` is an effective learning algorithm for modeling coordinated agents. Unlike `baller2vec`, `baller2vec++` can learn to emulate perfectly coordinated agents from a simulated toy dataset (Section 5.1). Further, `baller2vec++` outperforms `baller2vec` by a wide margin (8.9%) when modeling the trajectories of professional basketball players (Section 5.1).
2. `baller2vec++` makes better forecasts when conditioned on concurrent trajectory information from other agents, supporting our proposition that the commonly used independence assumption for agent trajectories is overly strong (Section 5.2).

²See the authors’ implementation here: https://github.com/ezhan94/multiagent-programmatic-supervision/blob/a1d9152d4c8a287474953cba093c28fef2a05979/models/macro_vrnn.py#L101.

3. Lastly, the joint probability assigned to a sequence by `baller2vec++` is approximately permutation invariant with respect to the order of the agents, i.e., `baller2vec++` respects the properties of the chain rule (Section 5.3).

2 Background

2.1 Multi-agent trajectory modelling

Our problem description closely follows Alcorn and Nguyen [6], whom we quote here:

Let $A = \{1, 2, \dots, B\}$ be a set indexing B agents and $P = \{p_1, p_2, \dots, p_K\} \subset A$ be the K agents involved in a particular sequence. [Let] $C_t = \{(x_{t,1}, y_{t,1}), (x_{t,2}, y_{t,2}), \dots, (x_{t,K}, y_{t,K})\}$ [be] an unordered set of K coordinate pairs such that $(x_{t,k}, y_{t,k})$ are the coordinates for agent p_k at time step t . The ordered sequence of sets of coordinates $\mathcal{C} = (C_1, C_2, \dots, C_T)$, together with P , thus defines the trajectories for the K agents over T time steps.

In multi-agent trajectory modeling, the goal is to model a joint probability of the form:

$$p(\Delta x_{t,1}, \Delta x_{t,2}, \dots, \Delta x_{t,K} | x_{1:t,1}, x_{1:t,2}, \dots, x_{1:t,K})$$

i.e., the joint probability of the K agents’ trajectories $\Delta x_{t,k}$ at time step t given the agents’ location histories $x_{1:t,k}$. We note here that the common practice of *simultaneously* predicting the trajectories for all of the agents at a specific time step is not required by theory. Using the chain rule of probability, the joint probability of the agents’ trajectories can be factorized as, e.g.:

$$p(\Delta x_{t,1}, \Delta x_{t,2}, \dots, \Delta x_{t,K}) = p(\Delta x_{t,1})p(\Delta x_{t,2} | \Delta x_{t,1}) \dots p(\Delta x_{t,K} | \Delta x_{t,1}, \Delta x_{t,2}, \dots, \Delta x_{t,K-1})$$

where we omit the conditional historical trajectories for brevity. As a result, it is perfectly acceptable to generate trajectories agent-wise, using the previously generated trajectories as additional conditioning information when generating the trajectories for later agents (see Figure 2).

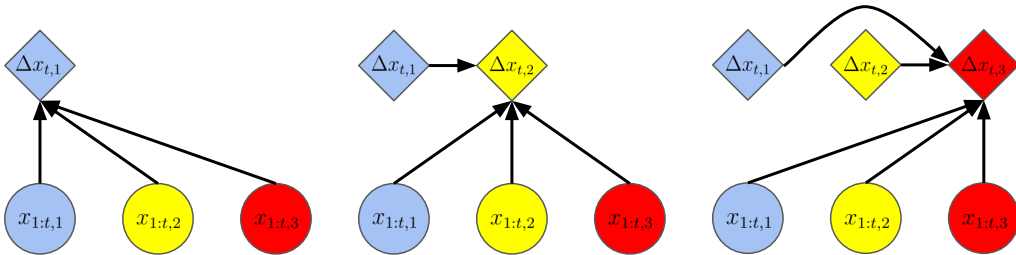


Figure 2: At inference time, a model is not *required* to *simultaneously* generate the trajectories for all of the agents at a specific time step. An alternative strategy is to allow the model to generate the agents’ trajectories one at a time, and let the model use the previously generated trajectories to inform the trajectories it generates for the remaining agents.

2.2 baller2vec is a (conditional) generative model.

`baller2vec` is a recently described *multi-entity* Transformer that can model sequences of *sets* (the underlying data structure for multi-agent spatiotemporal systems), as opposed to sequences of individual inputs (like words in a sentence). In the case of basketball, the input at each time step is a set of feature vectors where each feature vector contains information about the identity and location of a player on the court. `baller2vec` maps each input feature vector to an output feature vector, which is then used to “classify” the binned trajectory for that specific player at that specific time step.

Here, we provide a probabilistic interpretation of `baller2vec`, which establishes the theoretical grounds for using the chain rule to generate trajectories agent-wise at each time step in `baller2vec++`. Without loss of generality, we only consider one-dimensional trajectories for a single agent here. To briefly summarize, the outputs of the softmax function over the n binned trajectories in `baller2vec` can be interpreted as mixture proportions for a mixture of uniform distributions with predetermined bounds that partition the Euclidean trajectory space. Further, because $x_{t+1} = x_t + \Delta x_t$, `baller2vec` is in fact a conditional generative model that assigns a probability to a sequence of trajectories given the initial position of the agent, i.e., $p(\Delta x_1, \Delta x_2, \dots, \Delta x_T | x_1)$. Using the chain rule, we decompose the joint probability of the trajectories as:

$$p(\Delta x_1, \Delta x_2, \dots, \Delta x_T) = p(\Delta x_1) p(\Delta x_2 | \Delta x_1) \dots p(\Delta x_T | \Delta x_1, \Delta x_2, \dots, \Delta x_{T-1})$$

to reflect their temporal structure (we omit the conditional initial position term for brevity). Therefore, new trajectories can be generated from `baller2vec` with the following procedure (see Figure 3):

1. First, sample one of the n different mixture components using the mixture proportions output from the classifier f (i.e., `baller2vec`) conditioned on the agent’s current position, i.e., $i \sim \text{Categorical}(\pi_1, \pi_2, \dots, \pi_n)$ where $[\pi_1, \pi_2, \dots, \pi_n] = f(x_t)$.
2. Next, sample a trajectory from the uniform distribution associated with the sampled component, i.e., $\Delta x_t \sim \mathcal{U}(a_i, b_i)$.
3. Finally, add the sampled trajectory to the agent’s input position to generate the agent’s position at the start of the next time step, i.e., $x_{t+1} = x_t + \Delta x_t$.

Let $[\Delta x_{min}, \Delta x_{max})$ be an interval on the real line such that any trajectory $\Delta x < \Delta x_{min}$ or $\Delta x \geq \Delta x_{max}$ has zero density (i.e., such trajectories are humanly impossible). Let $\{[a_i, b_i]\}_{i=1}^n$ be a set of n intervals that partition the interval $[\Delta x_{min}, \Delta x_{max})$ into n bins, i.e., $\cup_{i=1}^n [a_i, b_i] = [\Delta x_{min}, \Delta x_{max})$ and $i \neq j \implies [a_i, b_i] \cap [a_j, b_j] = \emptyset$. Recall that the probability density function (PDF) for a uniform distribution with bounds $-\infty < a < b < \infty$ is:

$$p(\Delta x) = \begin{cases} \frac{1}{b-a} & \text{for } \Delta x \in [a, b) \\ 0 & \text{otherwise} \end{cases}$$

Letting $c_i = \frac{1}{b_i - a_i}$, the PDF for a mixture of uniforms with these bounds is thus:

$$p(\Delta x) = \sum_{i=1}^n \pi_i \mathcal{U}(\Delta x; a_i, b_i) = \sum_{i=1}^n \pi_i c_i \quad (1)$$

where $p(\Delta x)$ is the density assigned to Δx by the mixture, π_i is the mixture proportion for the mixture component indexed by i (i.e., $0 \leq \pi_i \leq 1$ and $\sum \pi_i = 1$), and $\mathcal{U}(\Delta x; a_i, b_i)$ is the density assigned to Δx by the uniform distribution with bounds $-\infty < a_i < b_i < \infty$. Because the bounds of the uniform distributions partition $[\Delta x_{min}, \Delta x_{max})$, Equation (1) reduces to:

$$p(\Delta x) = \pi_{i'} c_{i'}$$

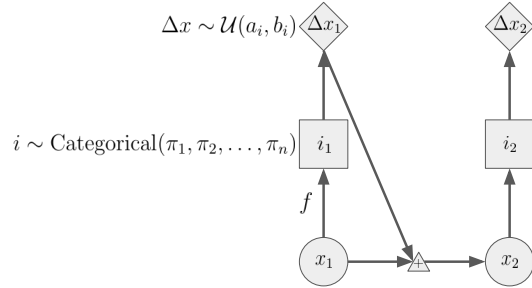


Figure 3: `baller2vec` can be viewed as a conditional generative model that assigns a probability to a sequence of trajectories given the initial positions of the agents. Here, we show a graphical model depiction of a `baller2vec` model that generates a sequence of one-dimensional trajectories for a single agent. Given the initial position of the agent (the circle containing x_1), one of n different uniform distributions (the square containing i_1) is sampled using the mixture proportions (π_i) output by `baller2vec` (f). The agent’s trajectory (the diamond containing Δx_1) is then sampled from the selected uniform distribution, which has bounds $-\infty < a_i < b_i < \infty$. At the start of the next time step, the agent’s position is $x_2 = x_1 + \Delta x_1$. Maximizing the likelihood of `baller2vec` as a classifier over the binned trajectories is thus equivalent to maximizing its likelihood when assuming the trajectories are generated from a mixture of uniform distributions that partition the Euclidean trajectory space (see Section 2.2 for details).

where $\Delta x \in [a_{i'}, b_{i'}]$ (because the other uniform distributions will assign a density of zero to Δx). The likelihood for data D (with $|D| = N$) is then:

$$\mathcal{L}(D) = \prod_{j=1}^N p(\Delta x_j) = \prod_{j=1}^N \pi_{j,i'} c_{j,i'}$$

where $\pi_{j,i'}$ is the mixture proportion assigned to the component with $\Delta x_j \in [a_{i'}, b_{i'}]$ and $c_{j,i'}$ is the associated density. Taking the negative logarithm of the likelihood gives:

$$-\ln(\mathcal{L}(D)) = -\sum_{j=1}^N \ln(\pi_{j,i'}) - \sum_{j=1}^N \ln(c_{j,i'}) \quad (2)$$

Because the bounds are fixed, the second summation is a constant, and Equation (2) becomes:

$$-\ln(\mathcal{L}(D)) = -\sum_{j=1}^N \ln(\pi_{j,i'}) + C$$

where $C = -\sum_{j=1}^N \ln(c_{j,i'})$. Therefore, minimizing the loss of `baller2vec` as a classifier of binned trajectories is equivalent to minimizing the loss of the model when assuming the trajectories are generated from a mixture of uniform distributions as specified in Equation (1).

3 Model Architecture

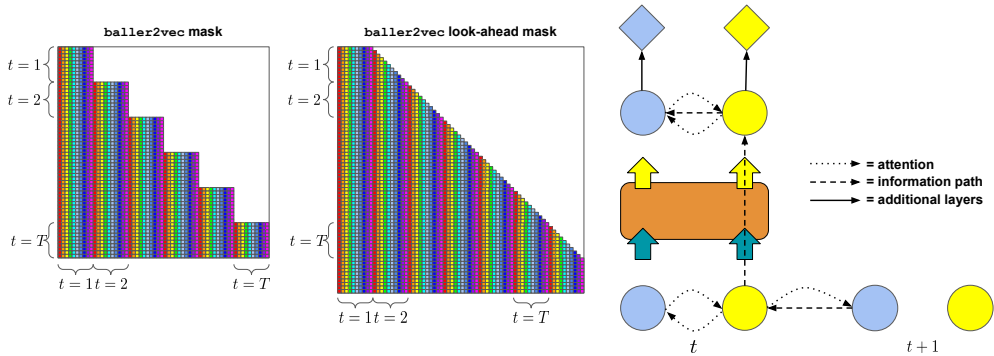


Figure 4: A naive strategy for learning to predict statistically dependent agent trajectories is to adapt the `baller2vec` self-attention mask so that `baller2vec` can “look ahead” at future positions of agents whose trajectories are generated *prior* to the agent being processed in the current time step. However, this look-ahead self-attention mask cannot be used with multi-layer Transformers because doing so necessitates “seeing the future”. For example, after the model attends to the blue agent’s position at time step $t + 1$ when processing the yellow agent at time step t , the yellow agent’s resultant feature vector contains information about the blue agent’s future position. As a result, when the model attends to the yellow agent while processing the blue agent at the next level, the model is seeing the future.

We motivate our `baller2vec++` architecture by first highlighting an issue that arises in `baller2vec` when trying to model agent trajectories using the chain rule. The `baller2vec` self-attention mask can be adapted so that `baller2vec` “looks ahead” at the future positions of agents whose trajectories are generated prior to the agent being processed in the current time step (Figure 4). However, this look-ahead self-attention mask can only be used with the final layer of the Transformer; otherwise, the model needs to see the future (Figure 4). As a result, `baller2vec` is severely limited in the conditional distribution functions it can learn.

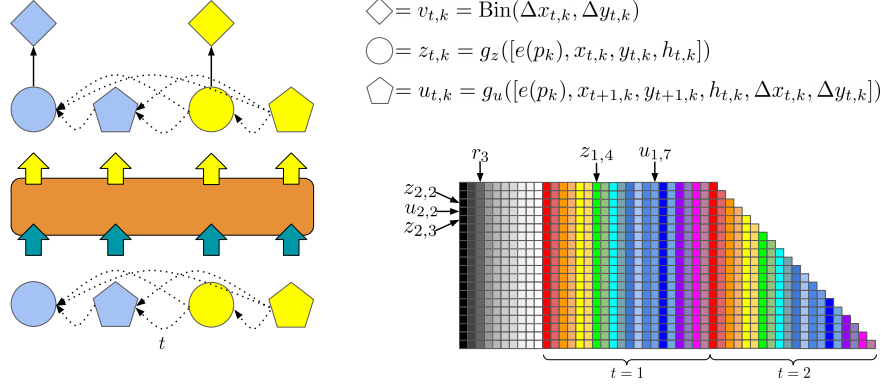


Figure 5: To learn statistically dependent agent trajectories, `baller2vec++` uses a specially designed self-attention mask to simultaneously process three different sets of features vectors in a single Transformer. The three sets of feature vectors consist of location feature vectors like those found in `baller2vec` ($z_{t,k}$), look-ahead trajectory feature vectors ($u_{t,k}$), and starting location feature vectors (r_k ; not shown). As can be seen in these partial depictions of `baller2vec++` and the `baller2vec++` self-attention mask, this design allows the model to integrate information about *concurrent* agent trajectories through *multiple* Transformer layers without seeing the future.

`baller2vec++` (Figure 5) overcomes this limitation by: (1) augmenting the `baller2vec` input with two other sets of feature vectors and (2) using a specially designed self-attention mask. The three sets of feature vectors in `baller2vec++` take the following forms:

1. $z_{t,k} = g_z([e(p_k), x_{t,k}, y_{t,k}, h_{t,k}])$ **(current location information)**
2. $u_{t,k} = g_u([e(p_k), x_{t+1,k}, y_{t+1,k}, h_{t,k}, \Delta x_{t,k}, \Delta y_{t,k}])$ **(“look-ahead” information)**
3. $r_k = g_r([e(p_k), x_{1,k}, y_{1,k}, h_{1,k}])$ **(initial location information)**

where g_z , g_u , and g_r are multilayer perceptrons (MLPs), e is an agent embedding layer, and $h_{t,k}$ is a vector of optional contextual features for agent p_k at time step t . $z_{t,k}$ is the same location feature vector used in `baller2vec` and contains information about a specific agent’s identity and the agent’s location at time step t . $u_{t,k}$ is a “look-ahead” trajectory feature vector that contains information about a specific agent’s identity, the agent’s location at the *next time step* $t + 1$, and the agent’s trajectory at time step t , i.e., $(x_{t+1,k} - x_{t,k}, y_{t+1,k} - y_{t,k})$. Lastly, r_k is a starting location feature vector that contains information about a specific agent’s identity and the agent’s location at time step $t = 1$. The r_k feature vectors are necessary so that `baller2vec++` can “see” the initial locations of *all the agents* when processing the agents agent-wise in the first time step.

These three sets of feature vectors are combined to form a $(K + 2TK) \times F$ matrix Z such that the first K rows consist of the K r_k feature vectors, and the remaining $2TK$ rows consist of the TK $z_{t,k}$ and TK $u_{t,k}$ feature vectors interleaved with one another, i.e., each $z_{t,k}$ is followed by its corresponding $u_{t,k}$ in the matrix. This matrix is passed into the Transformer along with the specially designed self-attention mask, which encodes the following relationships (see Figure 5):

1. When processing r_{k_1} , `baller2vec++` is exclusively allowed to “look” at each r_{k_2} (i.e., `baller2vec++` cannot look at any location or look-ahead feature vectors when processing r_{k_1}).
2. When processing z_{t_2,k_2} , `baller2vec++` is allowed to “look” at: (i) each r_{k_1} , (ii) any z_{t_1,k_1} where (a) $t_1 < t_2$ **or** (b) $t_1 = t_2$ **and** $k_1 \leq k_2$, and (iii) any u_{t_1,k_1} where (a) $t_1 < t_2$ **or** (b) $t_1 = t_2$ **and** $k_1 < k_2$.
3. When processing u_{t_2,k_2} , `baller2vec++` is allowed to “look” at: (i) each r_{k_1} , (ii) any z_{t_1,k_1} where (a) $t_1 < t_2$ **or** (b) $t_1 = t_2$ **and** $k_1 \leq k_2$, and (iii) any u_{t_1,k_1} where (a) $t_1 < t_2$ **or** (b) $t_1 = t_2$ **and** $k_1 \leq k_2$.

Each processed $z_{t,k}$ feature vector is then passed through a linear layer followed by a softmax to classify the trajectory bin $v_{t,k}$ (where $v_{t,k} = \text{Bin}(\Delta x_{t,k}, \Delta y_{t,k})$ is an integer from one to n^2) for agent p_k at time step t . As with `baller2vec`, the loss for each sample is:

$$\mathcal{L} = \sum_{t=1}^T \sum_{k=1}^K -\ln(f(Z)_{t,k}[v_{t,k}]) \quad (3)$$

where $f(Z)_{t,k}[v_{t,k}]$ is the probability assigned to the trajectory bin $v_{t,k}$ by f , i.e., Equation (3) is the negative log-likelihood (NLL) of the data according to the model.

Because any ordering of a chain rule decomposition of a joint probability produces the same value, e.g.:

$$p(\Delta x_{t,1})p(\Delta x_{t,2}|\Delta x_{t,1})p(\Delta x_{t,3}|\Delta x_{t,1}\Delta x_{t,2}) = p(\Delta x_{t,3})p(\Delta x_{t,2}|\Delta x_{t,3})p(\Delta x_{t,1}|\Delta x_{t,3}\Delta x_{t,2})$$

like [11], we shuffled the order of the agents in each training sequence to encourage the model to learn joint probabilities of the agent trajectories that are permutation invariant with respect to the ordering of the agents.

4 Experiments

We tested `baller2vec++` on two different datasets. To highlight the pathological behavior of models that assume agent trajectories are statistically independent at each time step, we trained scaled down versions of `baller2vec++` and `baller2vec` on a toy dataset consisting of simulated trajectories for two perfectly coordinated agents. Additionally, to demonstrate the efficacy of `baller2vec++` in real world settings, we trained `baller2vec++` and `baller2vec` on a dataset of trajectories for professional basketball players.

4.1 Toy dataset

Each training sample was initialized with the agents starting at $(-1, 0)$ and $(1, 0)$ on a grid in random order (i.e., the first agent could be placed to either the left or the right of the origin). At each time step, one of nine actions (corresponding to the 3×3 grid surrounding the agent) was sampled from a uniform distribution, and each of the agents was translated along this trajectory. This process was repeated for 20 time steps (see Figure 6(a) for a sample).

4.2 Basketball dataset

We used the same National Basketball Association (NBA) dataset³ employed by Alcorn and Nguyen [6], whom we paraphrase here:

The NBA dataset consists of trajectories from 631 games from the 2015-2016 season, which were split into 569/30/32 training/validation/test games, respectively. During training, each sequence was sampled using the following procedure: (1) randomly select a training game, (2) randomly select a starting time from the game, (3) take the following four seconds of data and downsample it to 5 Hz from the original 25 Hz, and then (4) randomly (with a probability of 0.5) rotate the court 180° . This sampling procedure gave us access to on the order of ~ 82 million different (albeit overlapping) training sequences. For both the validation and test sets, $\sim 1,000$ different, *non-overlapping* sequences were selected for evaluation by dividing each game into $\lceil \frac{1,000}{N} \rceil$ non-overlapping chunks (where N is the number of games), and using the starting four seconds from each chunk as the evaluation sequence.

4.3 Model

Our `baller2vec++` and `baller2vec` models for the basketball dataset closely followed [6], and so largely resemble the original Transformer architecture [12]. Specifically, the Transformer settings

³<https://github.com/linouk23/NBA-Player-Movements>

were: $d_{\text{model}} = 512$ (the dimension of the input and output of each Transformer layer), eight attention heads, $d_{\text{ff}} = 2048$ (the dimension of the inner feedforward layers), six layers, no dropout, and no positional encoding. Each MLP (i.e., g_z , g_u , and g_r) had 128, 256, and 512 nodes in its three layers, respectively, and a ReLU nonlinearity following each of the first two layers. The player embeddings [13] had 20 dimensions, and $h_{t,k}$ was a binary variable indicating the side of the frontcourt for player p_k (i.e., the direction of his team’s hoop) at time step t . Lastly, the 11 ft \times 11 ft 2D Euclidean trajectory space was binned into 121 1 ft \times 1 ft squares.

We used the Adam optimizer [14] with an initial learning rate of 10^{-6} , $\beta_1 = 0.9$, $\beta_2 = 0.999$, and $\epsilon = 10^{-9}$ to update the model parameters, of which there were ~ 19 million. The learning rate was reduced to 10^{-7} after 20 epochs of the validation loss not improving. Models were implemented in PyTorch and trained on a single NVIDIA GTX 1080 Ti GPU for ~ 650 epochs (seven days) where each epoch consisted of 20,000 training samples, and the validation set was used for early stopping.

For the toy dataset, we used scaled down versions of the basketball models with $d_{\text{model}} = 128$, four attention heads, $d_{\text{ff}} = 512$, and two layers in the Transformer. Additionally, each MLP had two layers with 64 and 128 nodes, respectively. The models were trained for 50 epochs of 500 samples per epoch (~ 10.5 minutes) using a single learning rate of 10^{-5} .

5 Results

5.1 baller2vec++ can effectively model coordinated agents in both simulated and real settings

For the toy dataset, the training loss for baller2vec converged to $\sim 2.2 \approx -\ln(\frac{1}{9})$, i.e., the model was simply independently guessing the trajectories for both agents at every time step. In contrast, the training loss for baller2vec++ converged to $\sim 1.1 \approx -\ln(\frac{1}{9}) \div 2$, which is the expected loss for a model that perfectly learns the deterministic relationship between the agents’ trajectories (because the prediction for the second agent will always contribute $-\ln(1.0) = 0$ to the loss).

When generating trajectories with baller2vec, the agents are completely uncoordinated, with each agent following an independent random walk around the grid (Figure 6(b)). In contrast, trajectories generated by baller2vec++ display the same coordinated agent behavior as the training data (Figure 6(c)).

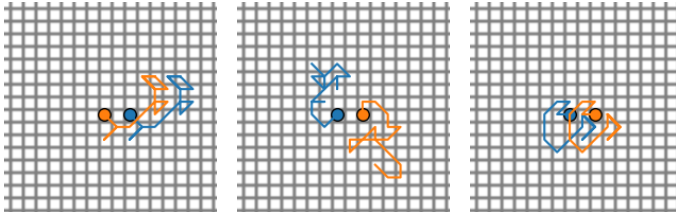


Figure 6: When trained on a dataset of perfectly coordinated agent trajectories (a), the trajectories generated by baller2vec are completely *uncoordinated* (b) while the trajectories generated by baller2vec++ are perfectly coordinated (c). Animated versions can be found in the code repository.

For the basketball dataset, baller2vec++ achieved an average NLL of 0.472 on the test set, 8.9% better than the average NLL for baller2vec (0.518). As can be seen in Figure 7, the trajectories generated by baller2vec++ are often more realistic than those generated by baller2vec. As was observed in [6], the trajectory forecast distributions for baller2vec become much more certain after observing a portion of the sequence (Figure 8), which suggests baller2vec may be inferring some of the shared hidden variables (e.g., plays) influencing the players. If that hypothesis was true, the performance gap between baller2vec++ and baller2vec should be largest at the beginning of the sequence (before any shared hidden variables can be inferred by baller2vec). Indeed, the average NLL for baller2vec++ in the *first time step* of each test set sequence (1.567) is 16.1% better than the average NLL for baller2vec (1.869), while the average NLL for baller2vec++ in the *last time step* of each test set sequence (0.420) is only 9.7% better than the average NLL for baller2vec (0.465) (see Figure 8).

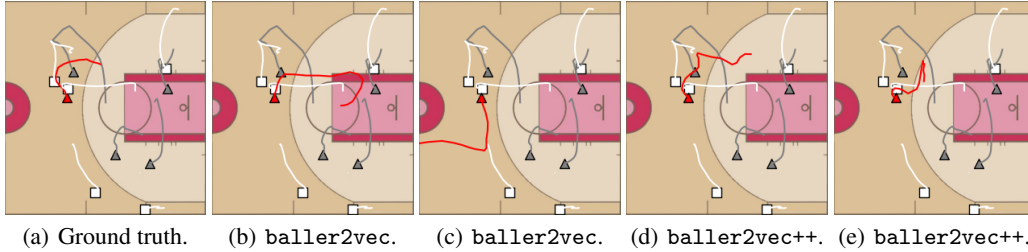


Figure 7: While `baller2vec` occasionally generates realistic trajectories for the red defender (b), it also makes egregious errors (c). In contrast, the trajectories generated by `baller2vec++` often seem plausible (d and e). For both the `baller2vec` and `baller2vec++` generated trajectories, the ground truth trajectories (a) for all of the non-red players were used as input at each time step. The red player was placed *last* in the player order when generating his trajectory with `baller2vec++`. Animated versions can be found in the code repository.

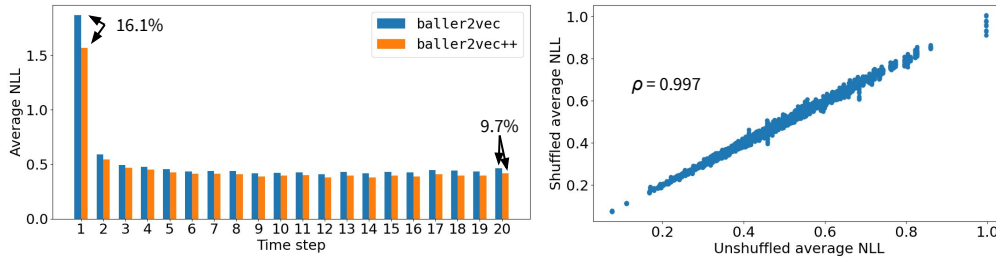


Figure 8: **Left:** when modeling the trajectories of professional basketball players, the performance gap between `baller2vec++` and `baller2vec` is largest at the beginning of the sequence, before shared unobserved variables can be inferred by `baller2vec`. Each bar indicates a model’s average NLL over the entire test set for that particular time step. For full sequences, `baller2vec++` outperforms `baller2vec` by 8.9%. **Right:** the joint probability assigned to a sequence by `baller2vec++` is approximately permutation invariant with respect to the order of the agents. For each point, its x value indicates `baller2vec++`’s average NLL for a test set sequence using the *original* order of the agents in the sequence, while its y value indicates `baller2vec++`’s average NLL for the *same* sequence with the order of the agents *shuffled*. The shuffled average NLLs are highly correlated with their corresponding unshuffled average NLLs.

5.2 baller2vec++ makes better forecasts when conditioned on concurrent trajectory information from other agents

Implicit in much of our discussion has been the intuition that providing a model with additional (relevant) information will improve its performance. To empirically test this conjecture, we compared the performance of `baller2vec++` when predicting the trajectory of a specific basketball player placed in the *first position* of the player order (i.e., when $k = 1$) vs. predicting the trajectory for that *same player* placed in the *last position* (i.e., when $k = 10$). Specifically, for each player in each test sequence, we calculated the NLL of the player’s trajectory in the first time step⁴ with the player in the *first position* of the player order. Next, we moved the player to the *last position* of the player order, and then randomly shuffled the remaining nine players 10 times, calculating the NLL for the player in the last position each time. Finally, we calculated the average percent change in the last position NLLs relative to their corresponding first position NLLs. On average, moving a player from the first to the last position improved the NLL for the player’s trajectory by 14.6%.

⁴Because, as previously discussed, the benefits of `baller2vec++` were most pronounced in the first time step.

5.3 The joint probability assigned to a sequence by `baller2vec++` is approximately permutation invariant with respect to the order of the agents

To determine whether or not `baller2vec++` respects the fact that any ordering of a chain rule decomposition of a joint probability produces the same value, we measured how much the average NLL for each test sequence in the basketball dataset varied when the order of the agents changed. Specifically, for each test set sequence, we shuffled the order of the agents 10 times. Then, for each permuted sequence, we calculated the percent error⁵ in the average NLL relative to the original, *unshuffled* sequence. Across all test sequences, the average percent error was only $\pm 1.5\%$. Further, as can be seen in Figure 8, the shuffled average NLLs are highly correlated with their corresponding unshuffled average NLLs (Pearson correlation coefficient = 0.997), i.e., the joint probability assigned to a sequence by `baller2vec++` is approximately permutation invariant with respect to the order of the agents.

6 Conclusion and Future Work

In this paper, we have shown how the commonly used independence assumption of many multi-agent spatiotemporal models can severely limit their ability to learn to emulate coordinated agents. By relaxing this independence assumption in `baller2vec`, `baller2vec++` was able to more accurately model the trajectories of professional basketball players. Models for other multi-agent spatiotemporal environments, such as pedestrian traffic (see [15] for a survey) and vehicle traffic (e.g., [16–19]), may also benefit from the look-ahead approach used by `baller2vec++`. Additionally, the interleaved input design of `baller2vec++` could be useful when modeling other systems involving many entities interacting through time, such as social media platforms (e.g., [20]). However, confronting the quadratic complexity of the Transformer attention mechanism as the number of entities grows large in these datasets is an open problem, but recent work in sparse Transformers (e.g., [21–24]) shows encouraging progress.

7 Acknowledgements

We would like to thank Jan Van Haaren for his helpful suggestions on how to improve the manuscript.

References

- [1] Panna Felsen, Patrick Lucey, and Sujoy Ganguly. Where will they go? predicting fine-grained adversarial multi-agent motion using conditional variational autoencoders. In *Proceedings of the European Conference on Computer Vision (ECCV)*, pages 732–747, 2018.
- [2] Agrim Gupta, Justin Johnson, Li Fei-Fei, Silvio Savarese, and Alexandre Alahi. Social gan: Socially acceptable trajectories with generative adversarial networks. In *Proceedings of the IEEE Conference on Computer Vision and Pattern Recognition*, pages 2255–2264, 2018.
- [3] Amir Sadeghian, Vineet Kosaraju, Ali Sadeghian, Noriaki Hirose, Hamid Reza Tofighi, and Silvio Savarese. Sophie: An attentive gan for predicting paths compliant to social and physical constraints. In *Proceedings of the IEEE/CVF Conference on Computer Vision and Pattern Recognition*, pages 1349–1358, 2019.
- [4] Raymond A Yeh, Alexander G Schwing, Jonathan Huang, and Kevin Murphy. Diverse generation for multi-agent sports games. In *Proceedings of the IEEE Conference on Computer Vision and Pattern Recognition*, pages 4610–4619, 2019.
- [5] Cunjun Yu, Xiao Ma, Jiawei Ren, Haiyu Zhao, and Shuai Yi. Spatio-temporal graph transformer networks for pedestrian trajectory prediction. In *Proceedings of the European Conference on Computer Vision (ECCV)*, August 2020.
- [6] Michael A. Alcorn and Anh Nguyen. `baller2vec`: A multi-entity transformer for multi-agent spatiotemporal modeling. *arXiv preprint arXiv:2102.03291*, 2021.

⁵See: https://en.wikipedia.org/wiki/Approximation_error#Formal_Definition.

- [7] Eric Zhan, Stephan Zheng, Yisong Yue, Long Sha, and Patrick Lucey. Generating multi-agent trajectories using programmatic weak supervision. In *International Conference on Learning Representations*, 2019. URL <https://openreview.net/forum?id=rkxw-hAcFQ>.
- [8] Stephan Zheng, Yisong Yue, and Jennifer Hobbs. Generating long-term trajectories using deep hierarchical networks. *Advances in Neural Information Processing Systems*, 29:1543–1551, 2016.
- [9] Vineet Kosaraju, Amir Sadeghian, Roberto Martín-Martín, Ian Reid, Hamid Rezaatofghi, and Silvio Savarese. Social-bigat: Multimodal trajectory forecasting using bicycle-gan and graph attention networks. In H. Wallach, H. Larochelle, A. Beygelzimer, F. d’Alché-Buc, E. Fox, and R. Garnett, editors, *Advances in Neural Information Processing Systems*, volume 32. Curran Associates, Inc., 2019. URL <https://proceedings.neurips.cc/paper/2019/file/d09bf41544a3365a46c9077ebb5e35c3-Paper.pdf>.
- [10] Petar Veličković, Guillem Cucurull, Arantxa Casanova, Adriana Romero, Pietro Liò, and Yoshua Bengio. Graph Attention Networks. *International Conference on Learning Representations*, 2018. URL <https://openreview.net/forum?id=rJXMpikCZ>. accepted as poster.
- [11] Zhilin Yang, Zihang Dai, Yiming Yang, Jaime Carbonell, Ruslan Salakhutdinov, and Quoc V Le. Xlnet: Generalized autoregressive pretraining for language understanding. *arXiv preprint arXiv:1906.08237*, 2019.
- [12] Ashish Vaswani, Noam Shazeer, Niki Parmar, Jakob Uszkoreit, Llion Jones, Aidan N Gomez, Łukasz Kaiser, and Illia Polosukhin. Attention is all you need. In *Advances in Neural Information Processing Systems*, pages 5998–6008, 2017.
- [13] Michael A Alcorn. (batter|pitcher)2vec: Statistic-free talent modeling with neural player embeddings. In *MIT Sloan Sports Analytics Conference*, 2018.
- [14] Diederik P Kingma and Jimmy Ba. Adam: A method for stochastic optimization. In *International Conference on Learning Representations*, 2015.
- [15] Andrey Rudenko, Luigi Palmieri, Michael Herman, Kris M Kitani, Dariu M Gavrila, and Kai O Arras. Human motion trajectory prediction: A survey. *The International Journal of Robotics Research*, 39(8):895–935, 2020.
- [16] Nachiket Deo and Mohan M Trivedi. Convolutional social pooling for vehicle trajectory prediction. In *Proceedings of the IEEE Conference on Computer Vision and Pattern Recognition Workshops*, pages 1468–1476, 2018.
- [17] Ming-Fang Chang, John Lambert, Patsorn Sangkloy, Jagjeet Singh, Slawomir Bak, Andrew Hartnett, De Wang, Peter Carr, Simon Lucey, Deva Ramanan, and James Hays. Argoverse: 3d tracking and forecasting with rich maps. In *Proceedings of the IEEE/CVF Conference on Computer Vision and Pattern Recognition (CVPR)*, June 2019.
- [18] Tianyang Zhao, Yifei Xu, Mathew Monfort, Wongun Choi, Chris Baker, Yibiao Zhao, Yizhou Wang, and Ying Nian Wu. Multi-agent tensor fusion for contextual trajectory prediction. In *Proceedings of the IEEE/CVF Conference on Computer Vision and Pattern Recognition (CVPR)*, June 2019.
- [19] Rohan Chandra, Uttaran Bhattacharya, Aniket Bera, and Dinesh Manocha. Taphic: Trajectory prediction in dense and heterogeneous traffic using weighted interactions. In *Proceedings of the IEEE/CVF Conference on Computer Vision and Pattern Recognition (CVPR)*, June 2019.
- [20] Emanuele Rossi, Ben Chamberlain, Fabrizio Frasca, Davide Eynard, Federico Monti, and Michael Bronstein. Temporal graph networks for deep learning on dynamic graphs. In *ICML 2020 Workshop on Graph Representation Learning*, 2020.
- [21] Rewon Child, Scott Gray, Alec Radford, and Ilya Sutskever. Generating long sequences with sparse transformers. *arXiv preprint arXiv:1904.10509*, 2019.

- [22] Manzil Zaheer, Guru Guruganesh, Kumar Avinava Dubey, Joshua Ainslie, Chris Alberti, Santiago Ontanon, Philip Pham, Anirudh Ravula, Qifan Wang, Li Yang, and Amr Ahmed. Big bird: Transformers for longer sequences. In H. Larochelle, M. Ranzato, R. Hadsell, M. F. Balcan, and H. Lin, editors, *Advances in Neural Information Processing Systems*, volume 33, pages 17283–17297. Curran Associates, Inc., 2020. URL <https://proceedings.neurips.cc/paper/2020/file/c8512d142a2d849725f31a9a7a361ab9-Paper.pdf>.
- [23] Iz Beltagy, Matthew E Peters, and Arman Cohan. Longformer: The long-document transformer. *arXiv preprint arXiv:2004.05150*, 2020.
- [24] Nikita Kitaev, Lukasz Kaiser, and Anselm Levskaya. Reformer: The efficient transformer. In *International Conference on Learning Representations*, 2020. URL <https://openreview.net/forum?id=rkgNKkHtvB>.